The supercapacitive performances of Co(OH)$_2$/Ni(OH)$_2$ composites in lithium hydroxide solution: Selection of electrolyte and effect of weight ratio

Linghao Su*, Liangyu Gong, Jinglong Gao

College of Chemistry & Pharmaceutical Science, Qingdao Agricultural University, Qingdao, Shandong 266109, PR China

ABSTRACT

The supercapacitive performances of Co(OH)$_2$/Ni(OH)$_2$ composites in lithium hydroxide solution are investigated in detail. Cyclic voltammetries and galvanostatic charge/discharge measurements reveal that LiOH is the most suitable electrolyte for the composite electrodes among MOH (M = Li, Na and K). The redox behavior of the Co(OH)$_2$/Ni(OH)$_2$ composites different to that of the pure components shows that weight ratio of Co(OH)$_2$/Ni(OH)$_2$ exerts a great influence on the capacitive performances. After 1000 continuous charge/discharge cycles, the capacitance retention ratio for the composite electrode with the weight ratio of 2/3 is elevated from 41.6% to 88.2% compared with pure Ni(OH)$_2$ electrode, exhibiting improved long-life cyclability.

© 2012 Elsevier B.V. All rights reserved.

1. Introduction

With in-depth research and development of supercapacitors, faradaic pseudocapacitors [1–3] have attracted increasing attention in the recent years. Owing to their charge-storage mechanism of fast and reversible redox reactions, faradaic pseudocapacitors usually deliver much more capacitance than electric double layer capacitors, which makes them suitable candidates for the applications in power systems delivering significant energy, such as electric vehicles. Among all of transition metal oxides as well as electrically conducting polymers (ECPs) used as the electrode active materials in pseudocapacitors, ruthenium oxide (RuO$_2$) is the best because of its good electrical conductivity and specific capacitance up to 863 F g^{-1} [4]. However, high cost prevents RuO$_2$ from practical application while ECPs are easy to decay. Therefore, great efforts have been put on searching for new materials in order to substitute RuO$_2$.

Recently, the possibility of using nickel hydroxide [5–10] as alternative material for RuO$_2$ has been increasingly considered because Ni(OH)$_2$ with great theoretical capacity used to be extensively employed as electrode material in alkaline batteries. Unfortunately, much lower capacitance than its theoretical capacity is obtained when Ni(OH)$_2$ is used alone as active material for pseudocapacitor due to its semiconductor nature. Considering the

improving effect of Co(OH)$_2$ on the electrochemical performances of Ni(OH)$_2$ electrode in alkaline batteries [11,12], it will be a good idea to construct Co(OH)$_2$/Ni(OH)$_2$ composite electrode for pseudocapacitors.

To date, there have been several reports in the literature on the study of Co(OH)$_2$/Ni(OH)$_2$ composites as active materials for pseudocapacitors. Gupta et al. [13] have potentiostatically deposited nanostructured Co$_x$Ni$_{1-x}$ layered double hydroxides (LDHs) onto stainless steel electrodes with very high specific capacitances. Hu et al. [14] have found that Co$_{0.41}$Ni$_{0.59}$ LDHs, synthesized by a chemical co-precipitation route, have an optimum capacitance property.

On the other hand, it is worth mentioning that KOH solution is often used in alkaline pseudocapacitors while other electrolytes are ignored, such as LiOH and NaOH. Recently, LiOH has attracted more attention than before. Yuan et al. [15] have found the capacitive behavior of the MnO$_2$/AC capacitor in 1 M LiOH electrolyte is much better than in 1 M KOH electrolyte. Wang et al. [16] have shown that MnO$_2$ electrode can exhibit an excellent pseudocapacitive behavior in 1 M LiOH electrolyte with a specific capacitance of 317 F g^{-1} at 0.1 A g^{-1}. In our early research [17], a specific capacitance of 187 F g^{-1} for Co-Al layered double hydroxide (Co-Al LDH) in 1 M LiOH aqueous solution is obtained after 1000 charge–discharge cycles at a current of 2 A g^{-1}. These researches show LiOH may be another electrolyte suitable to pseudocapacitors. Bearing above consideration in mind, we have here studied the capacitive performances of Co(OH)$_2$/Ni(OH)$_2$ composites in 1 M LiOH solution. The motivation for the present study has been to find whether the supercapacitive performances of Co(OH)$_2$/Ni(OH)$_2$

---

* Corresponding author. Tel.: +86 532 86080442; fax: +86 532 86080213.
 E-mail address: qauslh@163.com (L. Su).

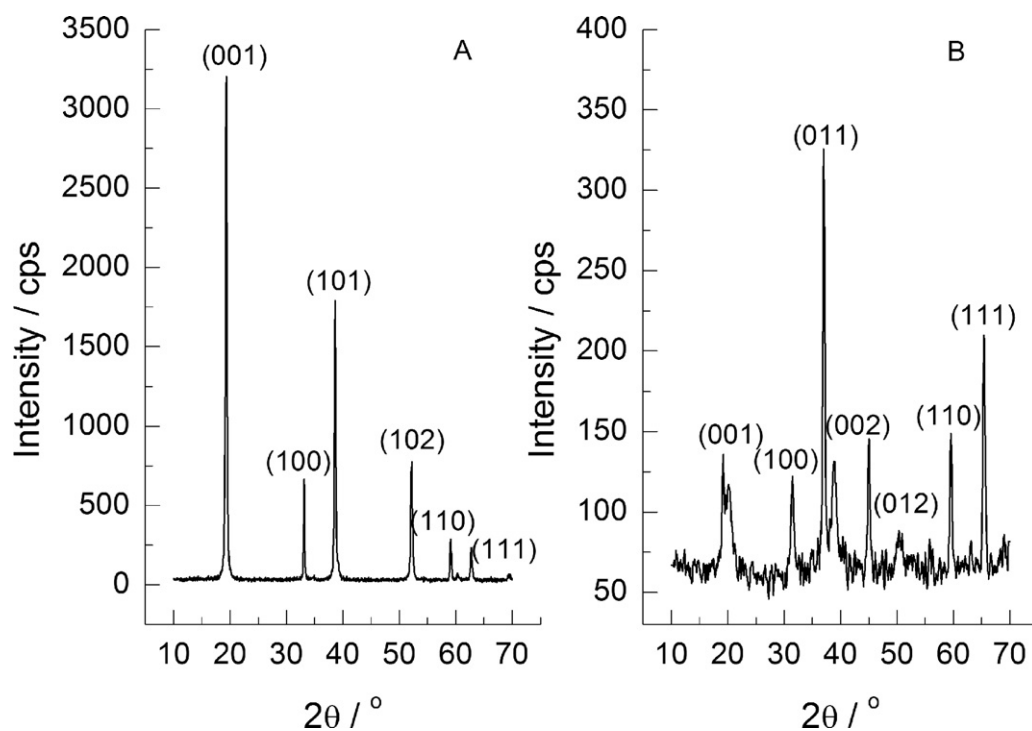**Fig. 1.** The XRD patterns of the as-synthesized (A) Ni(OH)$_2$ and (B) Co(OH)$_2$ materials.

composites are superior to the pure Ni(OH)$_2$ electrode in such a new alkaline electrolyte. We have also been interested in determining the effect of the weight ratio of Co(OH)$_2$/Ni(OH)$_2$ in the composites on the capacitive performances. Electrochemical measurements have demonstrated that Co(OH)$_2$/Ni(OH)$_2$ composites display a redox behavior different from the pure components (Co(OH)$_2$ and Ni(OH)$_2$), just like that described in the earlier literatures [13,14,18]. Meanwhile, a chief new observation in the work reported here is found that the composites perform optimum supercapacitive behaviors in 1 M LiOH solution among three MOH (M = Li, Na and K) alkaline electrolytes. Especially, the long-term cyclability of the Co(OH)$_2$/Ni(OH)$_2$ composite with an appropriate ratio is greatly improved as compared to the pure Ni(OH)$_2$ electrode.

2. Experimental

Ni(OH)$_2$ and Co(OH)$_2$ materials were synthesized by a low-temperature conversion method described elsewhere [19]. To testify the obtained materials, X-ray diffraction characterization and Fourier transform infrared spectra were performed on a D8 advance X-ray diffractometer using Cu Kα radiation (λ = 0.15418 nm) and a Nicolet IR200 spectrometer using KBr slice (sample/KBr weight ratio = 1/100), respectively.

The Co(OH)$_2$/Ni(OH)$_2$ composite electrodes were prepared according to the following procedures: mixing as-synthesized Co(OH)$_2$ and Ni(OH)$_2$ (in an appropriate weight ratio), acetylene black and polyterafluoroethylene with a weight ratio of 75:15:10 uniformly in an agate mortar, coating and pressing on a piece of foamed nickel of about 1 cm^2 (15 Mpa). A conventional three-electrode system was employed for the electrochemical measurements, equipped with a Pt foil of 1 cm^2 and a saturated calomel electrode (SCE) as counter and reference electrodes, respectively. The electrolyte used was 1 M LiOH, NaOH or KOH solution. Cyclic voltammetries and galvanostatic charge/discharge tests were carried out on a LK2005A-style electrochemical workstation and a Land CT2001A battery test system, respectively. Electrochemical

impedance spectra (EIS) were performed at 220 mV vs. SCE in 1 M LiOH solution with amplitude of 10 mV in the frequency range from 0.01 Hz to 100,000 Hz.

3. Results and discussion

Fig. 1 shows the XRD patterns of the as-synthesized Ni(OH)$_2$ and Co(OH)$_2$ materials. The diffractions at the 2θ values of 19.3°, 33.1°, 38.6°, 52.2°, 59.0° and 62.7° in Fig. 1A are typical for the hexagonal phase of Ni(OH)$_2$ (JCPDS: 14-0117) and are indexed to the (0 0 1), (1 0 0), (1 0 1), (1 0 2), (1 1 0) and (1 1 1) planes, respectively. The reflection peaks at the 2θ values of 19.2°, 31.5°, 36.9°, 50.4°, 59.5° and 65.4° shown in Fig. 1B, corresponding to the (0 0 1), (1 0 0), (0 1 1), (0 1 2), (1 1 0) and (1 1 1) planes, are ascribed to the hexagonal phase of Co(OH)$_2$ (JCPDS: 74-1057). These observations are in good accordance to the literature[19], confirming the formation of Ni(OH)$_2$ and Co(OH)$_2$.

The FTIR spectra shown in Fig. 2 also provides supporting information. The broad band at around 3400 cm^{-1} is the typical feature for the O–H stretching vibration of water molecules. The sharp vibration at 3644 cm^{-1} can be attributed to non-hydrogen bonded hydroxyl groups [20]. The absorption peak at about 1650 cm^{-1} is assigned to the bending model of water molecules. The low wave-number regions (600–400 cm^{-1}) are due to the M–OH cage vibrations [21]. As for the peaks at 2364 and 2386 cm^{-1}, they come from CO$_2$ in the air.

In order to select out a best electrolyte for Co(OH)$_2$/Ni(OH)$_2$ composite electrodes from three MOH (M = Li, Na and K) alkaline solutions, cyclic voltammetries and galvanostatic techniques are carried out. Fig. 3 shows the galvanostatic charge/discharge curves of the pure Ni(OH)$_2$ and Co(OH)$_2$ electrodes. There is a common feature that both Ni(OH)$_2$ and Co(OH)$_2$ electrodes perform better in 1 M LiOH than in the other two alkaline electrolytes, i.e., owning longer charge/discharge times (Table 1). Their CV curves also lead to the same conclusion. As shown in Fig. 4, the redox peak areas are larger in 1 M LiOH than in NaOH or KOH, suggesting that lithium hydroxide is the optimum electrolyte. So, 1 M LiOH solution was
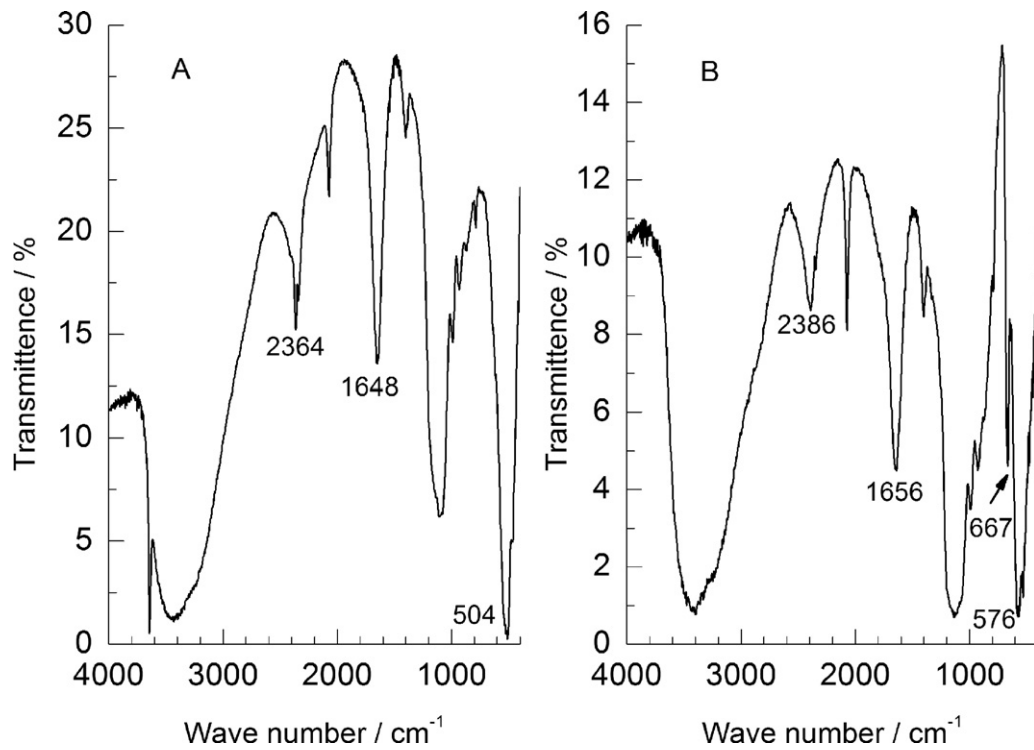
Fig. 2. The FTIR spectra of the as-synthesized (A) Ni(OH)$_2$ and (B) Co(OH)$_2$ materials.

selected as the electrolyte for Co(OH)$_2$/Ni(OH)$_2$ composite electrodes.

Fig. 5 shows the CV curves of Co(OH)$_2$/Ni(OH)$_2$ composite electrodes with the different weight ratio in 1 M LiOH solution at the scan rate of 2 mV s^{-1}. As the counterpart, pure Ni(OH)$_2$ electrode exhibits only one cathodic and one anodic peaks at 151 and 562 mV vs. SCE, respectively, responding to the redox reaction of Ni (II) ↔ Ni (III). Pure Co(OH)$_2$ electrode displays two cathodic and two anodic peaks at 65, 139, 223 and 393 mV vs. SCE, responding to the transformations of Co (II) ↔ Co (III) and Co (III) ↔ Co (IV), respectively.
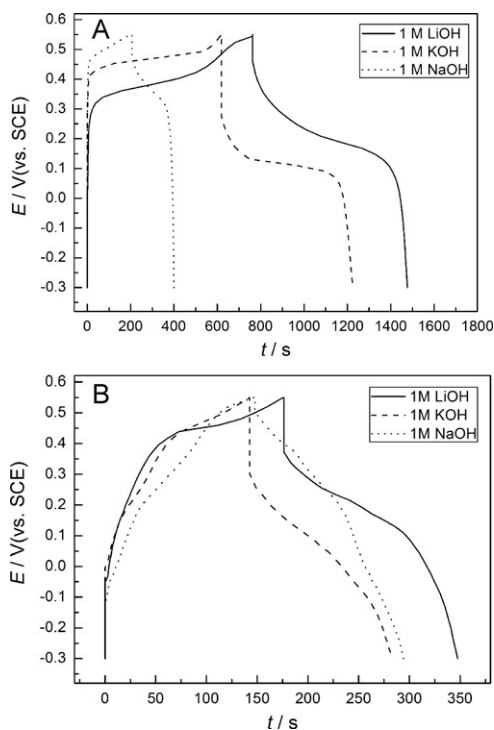

Fig. 3. Galvanostatic charge/discharge curves of the pure (A) Ni(OH)$_2$ and (B) Co(OH)$_2$ electrodes in different alkaline electrolytes at the current of 0.5 A g^{-1}.
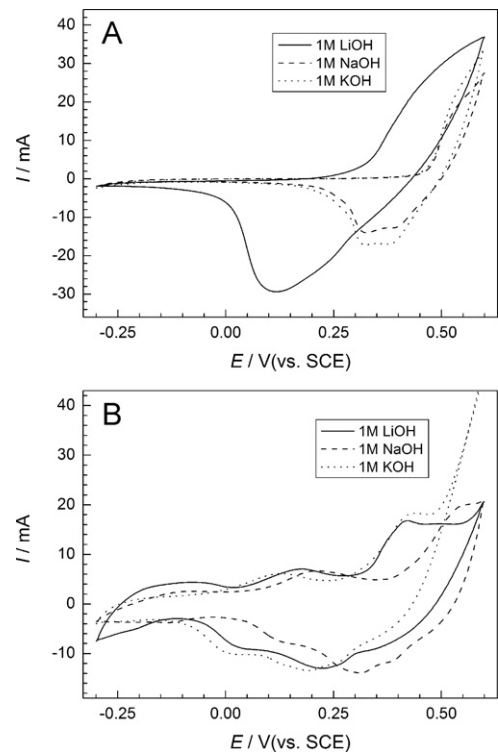

Fig. 4. Cyclic voltammograms of the pure (A) Ni(OH)$_2$ and (B) Co(OH)$_2$ electrodes in different alkaline electrolytes at a scan rate of 5 mV s^{-1}.

Table 1
Galvanostatic charge/discharge results of $Ni(OH)_2$ and $Co(OH)_2$ electrodes in different alkaline electrolytes at the current of $0.5\,A\,g^{-1}$.

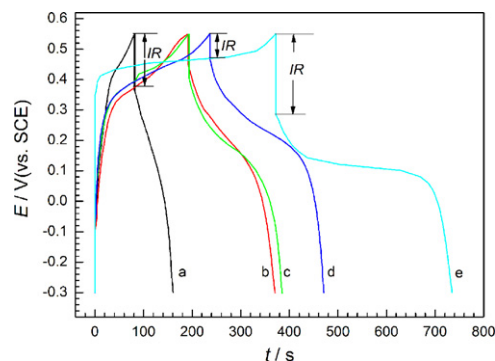| Electrode	Electrolyte	Charge time(s)	Disharge time(s)	Coulombic efficiency (%)
$Ni(OH)_2$	1 M LiOH	762.8	714.5	93.7
	1 M NaOH	619.3	606.2	97.9
	1 M KOH	206.1	193.8	94.0
$Co(OH)_2$	1 M LiOH	176.2	171.4	97.3
	1 M NaOH	142.6	141.2	99.0
	1 M KOH	147.6	146.6	99.3
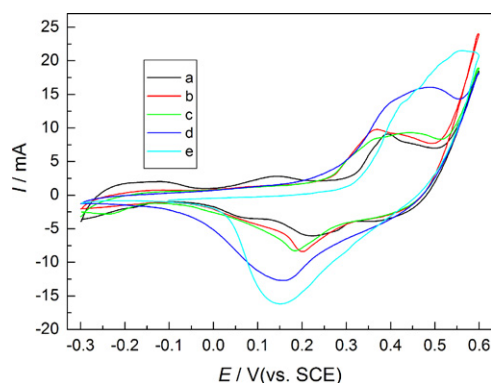
Fig. 5. Cyclic voltammograms of $Co(OH)_2/Ni(OH)_2$ composite electrodes in 1 M LiOH solution at $2\,mV\,s^{-1}$. $Co(OH)_2/Ni(OH)_2$ weight ratio: (a) 1:0, (b) 9:1, (c) 4:1, (d) 3:2 and (e) 0:1.

Fig. 6. Galvanostatic charge/discharge curves of $Co(OH)_2/Ni(OH)_2$ composite electrodes in 1 M LiOH solution at $1\,A\,g^{-1}$. $Co(OH)_2/Ni(OH)_2$ weight ratio: (a) 1:0, (b) 9:1, (c) 4:1, (d) 3:2 and (e) 0:1.

As for the $Co(OH)_2/Ni(OH)_2$ composite electrodes are concerned, only one cathodic and one anodic peaks are detected in their cyclic voltammograms. Furthermore, their peak potentials are different to that of the pure $Ni(OH)_2$ electrode. These observations are similar to that in the literature [18], indicating the interaction between $Ni(OH)_2$ and $Co(OH)_2$ in the composite. For the convenience of comparison, the peak positions are listed in Table 2, in which ΔE and E_f are defined as the average and difference between anodic and cathodic peak potentials ($E_{a,p}$ and $E_{c,p}$), respectively. As the content of $Co(OH)_2$ in the composite increases, the average potential E_f shifts negatively from $Ni(OH)_2$ to $Co(OH)_2$, showing the effect of the weight ratio on the electrochemical performance of $Ni(OH)_2$. Meanwhile, peak potential difference ΔE, indexing the reversibility of electrode reaction, gradually decreases and approaches to that of the pure $Co(OH)_2$ electrode, companying with the increase of the content of $Co(OH)_2$. These observations show that the electrochemical performances of $Co(OH)_2/Ni(OH)_2$ composite electrodes are superior to the pure $Ni(OH)_2$ electrode. In addition, the redox peak areas in their CV curves for composite electrodes are larger than that of the pure $Co(OH)_2$ electrode, in particular, for the composite with the weight ratio of 3:2.

The galvanostatic charge/discharge curves of the composite electrodes in 1 M LiOH at $1\,A\,g^{-1}$ are shown in Fig. 6. Compared with the pure $Ni(OH)_2$ and $Co(OH)_2$ electrodes, one of the remarkable differences is that the $Co(OH)_2/Ni(OH)_2$ electrodes display fewer pronounced IR drops, in particular, for the case with the weight

ratio of 3:2. This potential drop is caused by the overall internal resistance of the electrode. Namely, the charge-transfer resistance of the electrode can be decreased by constructing $Co(OH)_2/Ni(OH)_2$ composite electrodes. Another difference is the charge/discharge profiles of the composites are more like linear curves, more closing to the ideally symmetric straight-line charge/discharge profiles of RuO_2 or carbon-based materials, though their charge/discharge times are shorter than that of the pure $Ni(OH)_2$ electrode.

Fig. 7 plots the discharge specific capacitances (C_s) of various electrodes at different current densities in 1 M LiOH solution. The pure $Co(OH)_2$ electrode reveals the smallest specific capacitances while pure $Ni(OH)_2$ electrode displays the largest. For the composite electrodes, their specific capacitances are between the two pure-component electrodes. Nevertheless, their coulombic efficiencies (89.3–99.6%) are not inferior to the pure $Ni(OH)_2$ electrode (97.6–98.2%), as shown in Table 3. Moreover, the weight ratio exerts a great effect on their capacitance. When the weight ratio reaches to 3:2, the composite electrode delivers upmost capacitance, especially at heavy current densities ($226\,F\,g^{-1}$ at $2\,A\,g^{-1}$). These results are consistent with the observations in CV curves (Fig. 5) and galvanostatic charge/discharge curves (Fig. 6).

Table 2
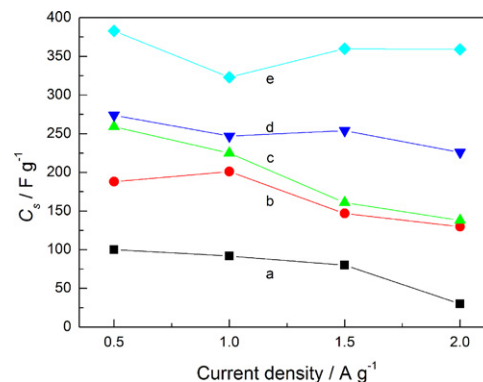Results of cyclic voltammetric measurements for $Co(OH)_2/Ni(OH)_2$ composite electrodes in 1 M LiOH solution at $2\,mV\,s^{-1}$.

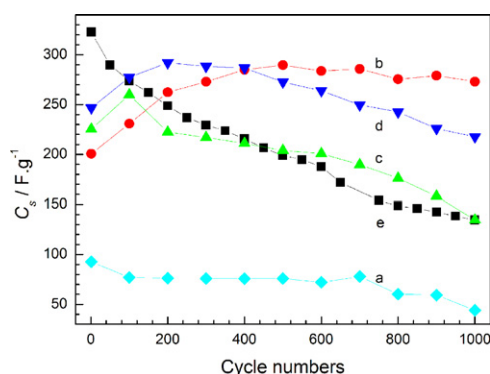| $Co(OH)_2/Ni(OH)_2$ weight ratio	$E_{a,p}$ (mV)	$E_{c,p}$ (mV)	ΔE (mV)	E_f (mV)
1:0	223	65	158	144
	393	139	254	266
9:1	369	201	168	285
4:1	441	185	256	313
3:2	487	159	328	323
0:1	562	151	411	356

Fig. 7. Specific capacitances of various electrodes at different current densities. $Co(OH)_2/Ni(OH)_2$ weight ratio: (a) 1:0, (b) 9:1, (c) 4:1, (d) 3:2 and (e) 0:1.

Table 3
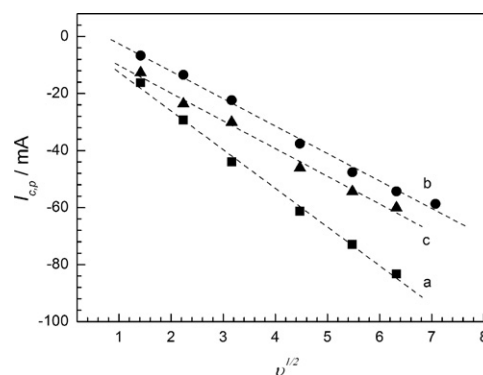Coulombic efficiency of various composite electrodes at different current (%).

J (A g^{-1})	Co(OH)$_2$/Ni(OH)$_2$ weight ratio				
	1:0	9:1	4:1	3:2	0:1
0.5	95.8	94.9	89.9	95.8	98.2
1.0	97.9	89.3	98.7	98.8	98.2
1.5	90.9	93.6	99.4	97.7	97.6
2.0	94.9	97.0	99.3	99.6	98.1

The charge/discharge cyclability of the composite electrodes in 1 M LiOH solution was carried out at the current density of 1 A g^{-1} and the relation of discharge specific capacitance to the cyclic number is plotted in Fig. 8. With increasing cyclic number, the specific capacitance of the pure Ni(OH)$_2$ electrode decreases dramatically from 322 F g^{-1} to 134 F g^{-1} with a retention of 41.6% after 1000 continuous cycles. Pure Co(OH)$_2$ electrode performs almost in the same way as Ni(OH)$_2$ with a capacitance retention of 47.4%. For composite electrodes, however, an obvious characteristic is that they all undergo an increasing step of specific capacitance within first several hundred cycles, then followed by a decreasing step. Even so, their capacitance retention ratio for the composite electrodes is still much larger than the two pure component ones after 1000 continuous charge/discharge cycles. For example, for the case of the weight ratio at 3:2, it is up to 88.2%, which is comparable to the reported value in the literature [14].

In order to explain the improving effect of added Co(OH)$_2$ on the electrocapacitive properties of Ni(OH)$_2$ electrode, we carried out a series of cyclic voltammetry at various scan rates in 1 M LiOH solution for pure Ni(OH)$_2$, Co(OH)$_2$ and composite (with the weight ratio of 3:2) electrodes. Because the anodic peaks are difficult to detect in their CV curves, Fig. 9 only provides the relations of cathodic peak current ($I_{c,p}$) to scan rate (v). The composite electrode displays the same linear feature as the two pure component electrodes, i.e., $I_{c,p}$ increasing with $v^{1/2}$ proportionately, confirming that the Co(OH)$_2$/Ni(OH)$_2$ electrode still undergoes the diffusion-control kinetic process like Ni(OH)$_2$ and Co(OH)$_2$ electrodes. Thereby, the enhancement of the composite electrode can be attributed to the improvement of the electrode's charge-transfer process by adding Co(OH)$_2$ in Ni(OH)$_2$. This point is clearly seen from the electrochemical impedance spectra (EIS) shown in Fig. 10. The semicircle in the high-frequency region is related to the charge-transfer process, and its diameter is charge-transfer resistance. In the middle frequency region, it displays a spike characteristic of capacitive behavior. Compared with the pure Ni(OH)$_2$ electrode, the composite electrode with the weight ratio of 3:2 reduces its charge-transfer resistance effectively.

Fig. 9. Dependence of cathodic peak current ($I_{c,p}$) on scan rate (v) for the three electrodes in 1 M LiOH solution. (a) pure Ni(OH)$_2$, (b) pure Co(OH)$_2$ and (c) composite electrode at weight ratio of 3:2.
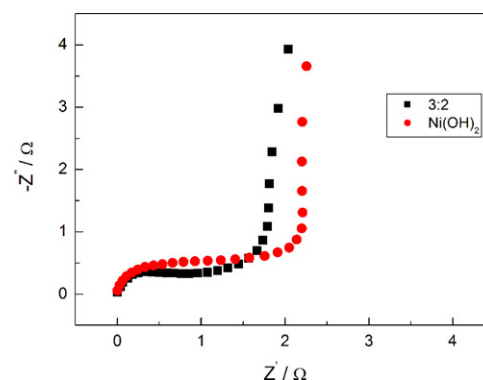
Fig. 10. EIS spectra of the pure Ni(OH)$_2$ and composite electrodes in 1 M LiOH solution.

4. Conclusions

Lithium hydroxide is selected as the electrolyte suitable for Co(OH)$_2$/Ni(OH)$_2$ composite electrodes by comparing the electrochemical performances in 1 M LiOH, NaOH and KOH solution. The weight ratio of Co(OH)$_2$/Ni(OH)$_2$ in the composite electrodes has great influence on their supercapacitive behavior. After 1000 continuous charge/discharge cycles, the capacitance–retention ratio increases from 41.6% (for the pure Ni(OH)$_2$ electrode) to 88.2% (for the composite electrode with the weight ratio of 3:2). EIS spectra shows that the improvement effect is due to the decrease of the electrode's charge-transfer resistance though the composite electrode has the same kinetic feature of diffusion-control as Ni(OH)$_2$.

Acknowledgements

Fig. 8. Cyclability of various electrodes at the current of 1 A g^{-1} in 1 M LiOH solution. Co(OH)$_2$/Ni(OH)$_2$ weight ratio: (a) 1:0, (b) 9:1, (c) 4:1, (d) 3:2 and (e) 0:1.

References

[1] B.E. Conway, V. Birss, J. Wojtowicz, J. Power Sources 66 (1997) 1–14.
[2] J.P. Zheng, T.R. Jow, J. Electrochem. Soc. 142 (1995) L6–L8.
[3] A.K. Cuentas-Gallegos, M. Lira-Cantu, N. Casan-Pastor, P. Gomez-Romero, Adv. Funct. Mater. 15 (2005) 1125–1133.
[4] H. Kim, B.N. Popov, J. Power Sources 104 (2002) 52–61.
[5] E.E. Kalu, T.T. Nwoga, V. Srinivasan, J.W. Weidner, J. Power Sources 92 (2001) 163–167.
[6] D.D. Zhao, S.J. Bao, W.J. Zhou, H.L. Li, Electrochem. Commun. 9 (2007) 869–874.
[7] J. Chang, M. Park, D. Ham, S.B. Ogale, R.S. Mane, S.H. Han, Electrochim. Acta 53 (2008) 5016–5021.

[8] U.M. Patil, K.V. Gurav, V.J. Fulari, C.D. Lokhande, O.S. Joo, J. Power Sources 188 (2009) 338–342.
[9] H. Wang, H.S. Casalongue, Y. Liang, H. Dai, J. Am. Chem. Soc. 132 (2010) 7472–7477.
[10] J. Zhang, L.B. Kong, J.J. Cai, H. Li, Y.C. Luo, L. Kang, Micropor. Mesopor. Mater. 132 (2010) 154–162.
[11] R.D. Armstrong, E.A. Charles, J. Power Sources 25 (1989) 89–97.
[12] P. Elumalai, H.N. Vasan, N. Munichandraiah, J. Power Sources 93 (2001) 201–208.
[13] V. Gupta, S. Gupta, N. Miura, J. Power Sources 175 (2008) 680–685.
[14] Z.A. Hu, Y.L. Xie, Y.X. Wang, H.Y. Wu, Y.Y. Yang, Z.Y. Zhang, Electrochim. Acta 54 (2009) 2737–2741.

[15] A. Yuan, Q. Zhang, Electrochem. Commun. 8 (2006) 1173–1178.
[16] X. Wang, A. Yuan, Y. Wang, J. Power Sources 172 (2007) 1007–1011.
[17] L.H. Su, X.G. Zhang, C.H. Mi, Y. Liu, J. Power Sources 179 (2008) 388–394.
[18] J. Ismail, M.F. Ahmed, P. Vishnu Kamath, J. Power Sources 41 (1993) 223–230.
[19] X.L. Li, J.F. Liu, Y.D. Li, Mater. Chem. Phys. 80 (2003) 222–227.
[20] V. Gupta, T. Kusahara, H. Toyama, S. Gupta, N. Miura, Electrochem. Commun. 9 (2007) 2315–2319.
[21] M. Rajamathi, P.V. Kamath, R. Seshadri, Mater. Res. Bull. 35 (2000) 271–278.